HHS Public Access

Author manuscript

Nature. Author manuscript; available in PMC 2011 December 02.

Published in final edited form as:

Nature. 2011 June 2; 474(7349): 109–113. doi:10.1038/nature09971.

Substrate-modulated gating dynamics in a Na+-coupled neurotransmitter transporter homolog

Yongfang Zhao[1,2,4,7], **Daniel Terry**[5,7], **Lei Shi**[5,6,7], **Matthias Quick**[1,2,4], **Harel Weinstein**[5,6,☎], **Scott C. Blanchard**[5,☎], and **Jonathan A. Javitch**[1,2,3,4,☎]

[1]Center for Molecular Recognition, Columbia University College of Physicians and Surgeons, 630 W. 168th, New York, New York 10032, USA

[2]Department of Psychiatry, Columbia University College of Physicians and Surgeons, 630 W. 168th, New York, New York 10032, USA

[3]Department of Pharmacology, Columbia University College of Physicians and Surgeons, 630 W. 168th, New York, New York 10032, USA

[4]Division of Molecular Therapeutics, New York State Psychiatric Institute, New York, NY 10032, USA

[5]Department of Physiology and Biophysics, Weill Medical College of Cornell University, 1300 York Avenue, New York, NY 10021, USA

[6]HRH Prince Alwaleed Bin Talal Bin Abdulaziz Alsaud Institute for Computational Biomedicine, Weill Cornell Medical College, Cornell University, 1300 York Avenue, New York, NY 10021, USA

Neurotransmitter:Na^+ symporters (NSS) terminate neuronal signaling by recapturing neurotransmitter released into the synapse in a co-transport (symport) mechanism driven by the Na^+ electrochemical gradient[1-6]. NSS for dopamine, norepinephrine, and serotonin are targeted by the psychostimulants cocaine and amphetamine[1], as well as by antidepressants[7]. The crystal structure of LeuT, a prokaryotic NSS homolog, revealed an occluded conformation in which a leucine (Leu) and two Na^+ ions are bound deep within the protein.[8] This structure has been the basis for extensive structural and computational exploration of the functional mechanisms of proteins with a LeuT-like fold[9-22]. Subsequently, an 'outward-

☎Jonathan A. Javitch, M.D., Ph.D., Columbia University College of Physicians and Surgeons, Center for Molecular Recognition, 630 West 168th Street, P&S 11-401, New York, NY 10032, USA; Phone: 212-305-7308; Facsimile: 212-305-5594; jaj2@columbia.edu. ☎ Scott C. Blanchard, Ph.D., Department of Physiology and Biophysics, Weill Cornell Medical College, Cornell University, 1300 York Avenue, New York, NY 10021, USA. Phone: 212-746-6163; Facsimile: 212-746-4843; scb2005@med.cornell.edu. ☎Harel Weinstein, D.Sc., Department of Physiology and Biophysics, Weill Cornell Medical College, Cornell University, 1300 York Avenue, New York, NY 10021, USA. Phone: (212) 746-6358; Facsimile: (212) 746-8690; haw2002@med.cornell.edu.

[7]These authors contributed equally.

Author Contributions: Y.Z. expressed, purified, and labeled the LeuT mutants. M.Q. and Y.Z. performed the functional characterization of the mutants. Y.Z. and D.T. designed, carried out, and analyzed the single-molecule experiments; L.S. and H.W. designed and analyzed the computational studies, which were carried out by L.S.; S.C.B. and J.A.J. helped design the biochemical and single-molecule experiments and, with L.S. and H.W., helped to interpret the data. All the authors contributed to writing and editing the manuscript.

Supplementary Information is linked to the online version of the paper at www.nature.com/nature

open' conformation was determined in the presence of the inhibitor tryptophan[23], and the Na^+-dependent formation of a dynamic outward-facing intermediate was identified using electron paramagnetic resonance spectroscopy[24]. In addition, we have used single-molecule fluorescence resonance energy transfer (smFRET) imaging to reveal reversible transitions to an inward-open LeuT conformation, that involve the movement of TM1a away from the transmembrane helical bundle[22]. Here, we have investigated how substrate binding is coupled to structural transitions in LeuT during Na^+-coupled transport, a process whereby substrate binding from the extracellular side of LeuT facilitates intracellular gate opening and substrate release at the intracellular face of the protein (Supplementary Fig. 1). In the presence of Ala, a substrate that is transported ∼10-fold faster than Leu[15],[25], we observed Ala-induced dynamics in the intracellular gate region of LeuT that directly correlate with transport efficiency. Collectively, our data reveal functionally-relevant and previously hidden aspects of the NSS transport mechanism that emphasize the functional importance of a second substrate (S2) binding site within the extracellular vestibule[15],[20]. Substrate binding in this S2 site appears to act cooperatively with the primary substrate (S1) binding site to control intracellular gating more than 30 Å away, in a manner that allows the Na^+ gradient to power the transport mechanism.

The experiments were performed on LeuT engineered to contain a 15 amino-acid, C-terminal biotinylation domain[26] and site-specifically labeled in the N-terminal loop (H7C, a position close to TM1) and IL1 (R86C) (**Methods**). Direct observations of conformational processes within the intracellular gate region of LeuT were made using a prism-based total internal reflection, wide field imaging strategy (Methods, Fig. 1a). As described[22], LeuT displays two readily-distinguished FRET states (∼0.51 and ∼0.75) in the presence of 200 mM K^+ and the nominal absence of Na^+ (Fig. 1b), consistent with the existence of two distinct conformations of the intracellular gate that differ by ∼13 Å in the distance separating the fluorophore pair.

In experiments imaging LeuT dynamics with increasing Na^+ concentrations, hidden Markov modeling (HMM) revealed that the distribution of low- and high-FRET conformations of LeuT was altered by Na^+ with an EC_{50} of 10.9 mM (Fig. 1b-c), consistent with the EC_{50} for Na^+-dependent stimulation of substrate binding and transport[15]. Na^+ decreased the overall frequency of transitions (Fig. 1d-e) through the preferential stabilization (∼7-fold) of the inward-closed state. During the direct imaging of individual LeuT molecules (Fig. 1f) slow, spontaneous transitions between open and closed states, initially observed in 200 mM K^+, were dramatically decreased upon exchange into Na^+-containing buffer, leading to the preferential stabilization of the inward-closed state.

Reasoning that substrate-induced intracellular gating might be observed best under conditions mimicking the relatively low intracellular Na^+, we performed experiments at Na^+ concentrations sufficient for Leu binding but below the EC_{50} of Na^+. However, even at 2 mM Na^+, Leu shifted the population toward the closed intracellular gate conformation (Supplementary Fig. 2a-b) through a ∼3.5-fold stabilization of this state (Supplementary Fig. 2c). These effects, which result in a global decrease in transition frequency (Supplementary Fig. 2d), were recapitulated at the level of individual LeuT molecules (Supplementary Fig. 2e). Thus, while unambiguously demonstrating binding of both Na^+

and Leu to LeuT, these results corroborate our earlier finding that Leu binding has the net effect of diminishing the likelihood of intracellular gate opening. One possible explanation for these observations is that Leu's high affinity for the transporter[15] makes it a poor substrate for transport, which in our measurements is manifested in the greatly extended lifetime of the closed state. To test this hypothesis, intracellular gate dynamics were assessed in the presence of the more efficiently transported substrate Ala.

In stark contrast to Leu, under otherwise identical conditions, increasing Ala concentrations did not shift the FRET distribution toward the closed state (Fig. 2a-b). Instead a strong, Ala concentration-dependent enhancement of transition rates was observed. In 2 mM Na^+, Ala enhanced the transition rates between inward-open and inward-closed states by as much as ∼4-fold (Fig. 2c-d). This result was directly confirmed at the scale of individual molecules upon exchange into Ala-containing buffer (Fig. 2e). Similar enhancements in transition frequency were also observed for H7C/T515C-LeuT (Supplementary Fig. 3). In accordance with such effects requiring both Na^+ and Ala, the lifetimes of the inward-open or inward-closed FRET states were not significantly affected by Ala alone (in the nominal absence of Na^+); at 250 μM Ala, the transition frequency increased in a Na^+ concentration-dependent fashion (Supplementary Fig. 4).

Using transition state theory (**Methods**) we found that the intracellular open and closed FRET states of LeuT were separated by a large activation barrier ($\Delta G^{\ddagger} \approx 80$ kJ/mol). Ala does not alter the relative occupancies of open and closed states but instead lowers the activation barrier for both open-to-closed and closed-to-open transitions by approximately 3 kJ/mol (on the order of a hydrogen bond). By contrast, Leu raised the activation barrier for the closed-to-open transition by as much as 4 kJ/mol – apparently through ground-state stabilization of the closed state.

Hypothesizing that the observed dynamics reflect Ala's acceleration of the opening-closing cycles of the intracellular gate required for the transport mechanism, we performed experiments in the presence of the transport inhibitor clomipramine (CMI), a tricyclic antidepressant that is known to bind in an extracellular vestibule above the Na^+ and S1 binding sites[25,27,28]. Many of the residues shown to interact with antidepressants in these structures are also part of the S2 site[25,27]. As substrate binding in the S2 site is thought to allosterically trigger intracellular release of Na^+ and substrate from the S1 site[15] (also see Supplementary Fig. 1), CMI should block Ala-induced intracellular gating dynamics. Indeed, in the presence of both Na^+ (10 mM) and Ala (250 μM), CMI essentially eliminated intracellular gate opening, stabilizing LeuT in a high-FRET, inward-closed conformation (Supplementary Fig. 5a-c). This observation is consistent with CMI competitively blocking substrate binding to the S2 site[15], thereby preventing Ala-induced opening and closing of the intracellular gate, and inhibiting transport. This result was again confirmed by direct imaging of individual LeuT molecules in Na^+ and Ala-containing buffer upon addition of CMI (Fig. 2f). The detergent n-octyl-β-D-glucopyranoside (OG) also inhibited intracellular gating dynamics (Supplementary Fig. 5a-c), consistent with its capacity to disrupt the Na^+-coupled transport mechanism[20] by competing with substrate binding to the S2 site[20,23].

To probe whether Ala binding to the S1 and/or S2 site(s) was responsible for lowering the activation barrier for intracellular gating dynamics, smFRET experiments were performed in the background of either an F253A or L400S mutation within the S1 or S2 site, respectively (Fig. 3a, Supplementary Fig. 1). These mutations disrupt substrate binding to LeuT, decreasing the stoichiometry of substrate binding under saturating conditions from 2 to 1 (Fig. 4a). Mutation of F253 blocks substrate binding to the S1 site and also abrogates transport (Fig. 4a-b; Supplementary Fig. 6), while having little or no effect on Na^+ binding (Supplementary Table 1). Despite evidence that Ala bound to the S2 site in the context of the F253A mutation (Fig. 4a), Ala failed to increase intracellular gating dynamics of the mutant protein (Fig. 4c). Similarly, despite evidence of Ala binding to the S1 site (Fig. 4a), no increase in intracellular gating dynamics was observed when the S2 site was disrupted by the L400S mutation (Fig. 4c). These findings support the notion that substrate occupancy in the S2 site is critical for the allosteric mechanism that controls intracellular gate opening and the release of substrate from the S1 site[15], and demonstrate that substrate binding to both the S1 and S2 sites is necessary to trigger intracellular gating.

In order to probe whether Ala binding to the S1 and S2 sites is also sufficient to promote intracellular gating and transport, experiments were performed in the presence of Li^+ in place of Na^+. In the presence of saturating Li^+ concentrations (>150 mM) we found that Ala binds LeuT with a 2:1 stoichiometry consistent with both S1 and S2 site occupancy (Fig. 4a). Li^+, like Na^+, stabilized the inward-closed state (Supplementary Fig. 7), but, in the presence of Li^+, Ala failed to accelerate intracellular gating dynamics and no substrate transport was observed (Fig. 4c). Instead, the inward-closed conformation of LeuT was modestly stabilized in the presence of Ala (∼2-fold reduction in the rate of gate opening, $k_{closed\text{-}open}$) (Fig. 4c). These data demonstrate that Ala binding to the S1 and S2 sites in the presence of Li^+ does not lower the activation barrier to intracellular gating as observed in the presence of Na^+.

Prompted by these experimental observations, computational studies were performed to investigate how both Na^+ and Li^+ can support substrate binding to LeuT, whereas only Na^+ leads to substrate-induced dynamics of the intracellular gate and to transport. These studies also served to identify local changes produced in the region of the ion binding sites and critical elements in the allosteric pathway linking the substrate binding sites and the intracellular gate region. Comparative analysis of separate molecular dynamics (MD) simulations of LeuT, performed with either Na^+ or Li^+ occupying the established Na^+ binding sites and in the absence of amino acid substrate (termed Na-only[24] and Li-only, respectively) revealed significant differences in TM-TM interactions (Fig. 3b-c), which are described in detail in the Supplementary Information. The Na1/Li1 binding site and its neighboring interaction network, which are crucial for the proper propagation of the allosteric effects from the S2 to S1 site (see Supplementary Information for details) and onward to the intracellular side to open the transport pathway, are sensitive to the unique combination of the ionic radius of the Na^+ cation and the charge redistribution it causes. The structural consequences of the ion-specific effects appear to be propagated through the cluster of aromatic residues at the heart of the S1 binding site, and result in different configurations of the bulge in the middle of TM10 (Fig. 3, Supplementary Fig. 8).

The positions of the structural elements involved in this propagation mechanism make them critical for transmitting conformational changes deeper into the TM bundle towards the intracellular end of the transporter (Fig. 3b-c). Such changes include local alterations in the vicinity of E419, a residue known from the crystal structure to interact with E62 in TM2, with the backbone of the unwound portion of TM6 (proximal to F259 of the aromatic cluster and the S1 binding site), and two water molecules[29]. Reconfiguration of this region, including residue T418, upon simulated inward movement of the substrate[15] was previously shown to enable the penetration of water from the intracellular side of LeuT as a result of an opening at IL1[15]. The resulting dissociation of IL1 from interactions with R5 and D369 and the destabilization of the network of intracellular interactions detected in the simulations (Supplementary Fig. 9) is associated with the observed outward movement of TM1a[22] that is essential for the simulated release of substrate to the intracellular side.

Due to the different effects of Li^+ and Na^+, Ala binding in both the S1 and S2 sites in the presence of Li^+ would not engender the ordered series of local conformational rearrangements expected in the presence of Na^+. These rearrangements originate in the S2 site and need to be propagated as described above through changes in the Na1 and S1 sites to enable water penetration from the cytoplasmic side of LeuT and the outward movement of TM1a. Their absence when Li^+ substitutes for Na^+ would explain why substrate-induced acceleration of gating dynamics was not observed experimentally.

Na^+ binding, which stabilizes the inward-closed state, does not hasten gate closure but, instead, slightly stabilizes the inward-open state as well, by raising the energy barrier to the conformational transition. In contrast, Ala binding to LeuT in the presence of Na^+ shortens not only the inward-closed, but also the inward-open lifetime (Fig. 2). Thus, bound Ala facilitates both the opening of the intracellular gate and its subsequent closure by reducing the activation barrier for such conformational transitions. One possible explanation for this observation is that binding of substrate in the S2 site triggers the opening of the intracellular gate and release of the S1 substrate to the cytoplasm. In the absence of S1 substrate and bound Na^+, substrate in the S2 site may then facilitate intracellular gate closure. It is tempting to speculate that the S2 substrate, in the presence of extracellular Na^+, may move to the S1 site with high efficiency due to its very high local concentration, thereby facilitating a subsequent transport cycle.

Collectively, our findings support the notion that the observed movements of TM1a and its environment are associated with LeuT intracellular gating[22] in a manner that is directly linked to the Na^+-driven transport mechanism. Thus, results obtained with the slowly transported substrate, Leu, and the relatively rapidly transported substrate, Ala, establish a relationship between the rates of intracellular gating and substrate transport. The role of substrate binding at the S2 site in the process of allostery and molecular recognition is further highlighted by the comparative effects of CMI and Ala binding to this site in the presence of Na^+. The former stabilizes a closed intracellular gate conformation, whereas the later substantially lowers the activation barrier to gate opening and thereby allows the energy of the Na^+ gradient to drive the transport mechanism.

While this manuscript was in review, a report was published that concluded, based on a variety of binding measurements, that LeuT has only a single high-affinity substrate site[30]. In contrast, our substrate binding measurements clearly show a stoichiometry of 2, consistent with high affinity binding to both the S1 and S2 sites. Half of this binding is lost in the S2-site mutant that also exhibits a loss of substrate-induced single-molecule dynamics and transport (Fig. 4). While the loss of substrate-induced dynamics and transport in the S2-site mutant could conceivably be explained solely by a long-range allosteric effect of the mutation, all our data to date are most consistent with a two-substrate-site model in which the absence of either S1 or S2 substrate binding results in a profound attenuation of transporter dynamics and function. We are currently uncovering the reasons for the discrepancy between the data published in Piscitelli *et al.*[30] and our own data, and will report our findings in due course.

Methods summary

LeuT mutants were expressed in *E. coli*, purified, and labeled on targeted engineered cysteines with Cy3 and Cy5 maleimide. The functional properties of the labeled constructs were determined by measuring Leu binding and Na^+ by scintillation proximity assay, and Ala transport was measured after reconstitution of the protein into proteoliposomes. Purified, labeled protein was immobilized onto a passivated-glass surface via a streptavidin-biotin linkage (schematized in Fig. 1a). Fluorescence data were acquired using a prism-based total internal reflection (TIR) microscope. Fluorescence resonance energy transfer (FRET) efficiency was calculated and analysis of fluorescence and FRET traces was achieved using automated analysis software developed for this application. The single molecule traces were analyzed for LeuT in the presence and absence of the substrates Na^+, Leu, and Ala, and upon addition of the transport inhibitors clomipramine and octylglucoside, and in response to mutations of the S1 and S2 binding sites. Molecular dynamics simulations were carried out with the protein immersed in an explicit membrane, solvated with water molecules, ions and ligands. Long equilibrations (totaling >2 μs) were run to assess conformational changes, with more than one MD trajectory collected for every configuration mentioned.

Methods

Protein expression and purification

LeuT variants were expressed in *E. coli* C41(DE3) as described[15]. For functional studies LeuT variants were expressed from pQO18 or derivatives thereof carrying the indicated mutations[20], whereas for single molecule FRET studies biotin acceptor peptide-tagged LeuT variants were expressed in pETO18G and its derivatives[22]. Protein was purified by immobilized metal (Ni^{2+}) affinity chromatography using a Ni^{2+} Sepharose 6 FastFlow column (GE Healthcare)[22]. For fluorescent labeling of LeuT, Cy3-maleimide and Cy5-maleimide (GE Healthcare) were added at an equimolar ratio (200 μM total) for 1 hour while the protein was bound to the Ni^{2+} resin[22]. Free dye was removed prior to the elution of LeuT with 300 mM imidazole.

Scintillation proximity-based binding studies

Binding of ^{3}H-leucine or ^{3}H-alanine (146 Ci/mmol and 49.4 Ci/mmol, respectively; both from Moravek) to purified LeuT-variants was measured with the scintillation proximity assay (SPA) as described[15] with 25 ng of purified protein per assay in buffer composed of 150 mM Tris/Mes, pH 7.5/50 mM NaCl/1 mM TCEP/0.1% n-dodecyl-β-D-maltopyranoside or 50 mM Tris/Mes, pH 7.5/150 mM LiCl/1 mM TCEP/0.1% n-dodecyl-β-D-maltopyranoside. To determine the molar ratio of Leu (or Ala)-to LeuT binding samples were incubated with increasing concentrations of radioligand and measured in the SPA cpm mode of the MircoBeta™ counter (Perkin Elmer). The efficiency of detection was calculated with standard curves of known concentrations of ^{3}H-Leu or ^{3}H-Ala. The standard curves were used to transform cpm into the amount of bound substrate[15]. The amount of LeuT in the SPA assays was determined[31]. SPA-based binding studies using 2 μM [^{22}Na]Cl (1017 mCi/mg; Perkin Elmer) were performed in 200 Tris/Mes, pH 7.5/1 mM TCEP/0.1% n-dodecyl-β-D-maltopyranoside in the presence of 0 – 50 mM NaCl (equimolar replacement of Tris/Mes to maintain a total molarity of 200 mM)[15]. All experiments were repeated at least in duplicate with triplicate determination of all individual data points. Kinetic constants (shown ± the SEM of the fit) were obtained by fitting the data of independent experiments to global fitting in Prism or SigmaPlot.

^{3}H-Ala transport in proteoliposomes

Proteoliposomes were prepared as described[15]. The accumulation of ^{3}H-Ala (49.4 Ci mmol^{-1}; Moravek) was measured at 23°C in assay buffer comprised of 150/50 mM Tris/Mes (pH 8.5) and 50 mM NaCl/150 mM LiCl. The reaction was quenched by the addition of ice-cold assay buffer without radiotracer and the proteoliposomes were collected on GF-75 glass fiber filters (Advantec) before the determination of the accumulated cpm by liquid scintillation counting.

Single-molecule FRET imaging experiments

Fluorescence experiments were performed using a prism-based TIRF microscope as previously described[22,32]. Microfluidic imaging chambers were passivated with a mixture of PEG and biotin-PEG and incubated with 0.8 μM streptavidin (Invitrogen). Cy3/Cy5-labeled, biotinylated LeuT molecules were surface immobilized through biotin-streptavidin interaction. Cy3 fluorophores were excited by the evanescent wave generated by TIR of a single-frequency light source (Ventus 532, Laser Quanta). Photons emitted from Cy3 and Cy5 were collected using a 1.2 N.A. 60× water-immersion objective (Nikon) and optical treatments were used to separate Cy3 and Cy5 frequencies onto a cooled, back-thinned EMCCD camera (Cascade 512, Photometrics). Fluorescence data were acquired using Metamorph (Universal Imaging Corporation).

All experiments were performed in buffer containing 50 mM Tris/Mes, pH 7.5, 10% glycerol, 0.02% (w/v) DDM, 5 mM 2-mercaptoethanol and 200 mM salt (KCl or NaCl, as specified). We used an oxygen-scavenging environment (1 unit per ml glucose oxidase, 8 units per ml catalase, 0.1% (v/v) glucose) containing 2 mM cyclooctatetraene in all experiments to minimize photobleaching.

Analysis of single-molecule fluorescence data was performed using custom software written in MATLAB (The MathWorks). A subset of the acquired traces was selected for further analysis using the following criteria: **1)** single-step donor photobleaching, **2)** signal-to-background noise ratio (SNR) ≥ 8, **3)** < 4 donor blinking events, **4)** non-zero FRET efficiency for at least 60 seconds. Additional manual trace selection was performed to refine the data, where selected traces were required to have: **1)** stable total fluorescence intensity (I_D+I_A) and **2)** at least one transition between clearly defined FRET states with anti-correlated transitions in donor/acceptor intensity or a single dwell in a clearly-defined FRET state. We found this process to be effective in removing artifacts and spurious noise without introducing significant bias (see Supplementary Discussion and Supplementary Figure 10). Kinetic analysis was performed to idealize FRET traces and calculate average dwell times using a three state model as previously described[22]. Error bars for transition rate estimates and FRET histograms were calculated as the standard deviation of 100 bootstrap samples of the traces. Error bars for state occupancies were calculated from 1,000 bootstrap samples.

Transition rates were interpreted using transition state theory, where the open and closed states are considered ground states separated by a large ($\Delta G^{\ddagger} \approx 80$ kJ/mol) activation barrier (the transition state). The energy required to achieve the transition state (and cross the barrier) was calculated as:

$$\Delta G^{\ddagger} = -\mathrm{RT}\ln\left(\frac{h \cdot k_{i,j}}{k_B T}\right),$$

where R is the gas constant, T is absolute temperature (296 K), *h* is Planck's constant, *k* is the measured transition rate, from state *i* to state *j* and k_B is Boltzmann's constant. Changes in the activation barrier energy ($\Delta\Delta G^{\ddagger}$) were calculated from the difference in forward and reverse rates observed in the absence and presence of substrate.

Molecular Dynamics

The Li^+-only simulation was performed on a system prepared as described[24]. Briefly, it consisted of over 77,000 atoms, including the explicit membrane model, solvating water molecules and the various ions and ligands. All the Na^+ ions in the system were replaced with Li^+. The parameters for Li^+ were from Noskov *et al.*[33]. All MD simulations were carried out with the NAMD program under constant temperature (310 K) and constant pressure (1 atm) (NPT) conditions. Long equilibration runs were performed to allow the system to transition to a new stable conformation. The inward-closed and inward-open conformations described in Supplementary Figure 9 were based on the simulations described previously[22]. More than one MD trajectory was collected for every configuration studied. Each individual trajectory was at least 360 ns, and the longest trajectory for each configuration was 720 ns. All the results reinforced the conclusions, and the structural and dynamic insights described in the main text were revealed as the common features and trends of parallel independent MD runs.

Supplementary Material

Refer to Web version on PubMed Central for supplementary material.

Acknowledgments

We thank R. Altman for assistance with reagents for single-molecule experiments and F. Carvalho for the preparation of membranes. Molecular graphic Figures and movies were prepared with PyMOL (DeLano Scientific; http://www.pymol.org). Computations were performed on Ranger at the Texas Advanced Computing Center (TG-MCB090022) and the David A. Cofrin computational infrastructure of the Institute for Computational Biomedicine at Weill Cornell Medical College. This work was supported in part by National Institutes of Health Grants DA17293 and DA022413 (J.A.J.), DA12408 (H.W.), DA023694 (L.S.), the Irma T. Hirschl/Monique Weill-Caulier Trusts (S.C.B.), and the Lieber Center for Schizophrenia Research and Treatment. D.S.T. is supported by the Tri-Institutional Training Program in Computational Biology and Medicine.

References

1. Amara SG, Sonders MS. Neurotransmitter transporters as molecular targets for addictive drugs. Drug Alcohol Depend. 1998; 51(1-2):87. [PubMed: 9716932]
2. Rudnick, Gary. Mechanisms of biogenic amine neurotransmitter transporters. 2. Humana Press Inc.; Totowa, New Jersey: 2002.
3. Sonders MS, Quick M, Javitch JA. How did the neurotransmitter cross the bilayer? A closer view. Curr Opin Neurobiol. 2005; 15(3):296. [PubMed: 15919190]
4. Gu H, Wall SC, Rudnick G. Stable expression of biogenic amine transporters reveals differences in inhibitor sensitivity, kinetics, and ion dependence. J Biol Chem. 1994; 269(10):7124. [PubMed: 8125921]
5. Torres GE, Gainetdinov RR, Caron MG. Plasma membrane monoamine transporters: structure, regulation and function. Nat Rev Neurosci. 2003; 4(1):13. [PubMed: 12511858]
6. Krause S, Schwarz W. Identification and selective inhibition of the channel mode of the neuronal GABA transporter 1. Mol Pharmacol. 2005; 68(6):1728. [PubMed: 16150932]
7. Iversen L. Neurotransmitter transporters and their impact on the development of psychopharmacology. Br J Pharmacol. 2006; 147(1):S82. [PubMed: 16402124]
8. Yamashita A, et al. Crystal structure of a bacterial homologue of Na^+/Cl^--dependent neurotransmitter transporters. Nature. 2005; 437(7056):215. [PubMed: 16041361]
9. Beuming T, Shi L, Javitch JA, Weinstein H. A comprehensive structure-based alignment of prokaryotic and eukaryotic neurotransmitter/Na^+ symporters (NSS) aids in the use of the LeuT structure to probe NSS structure and function. Mol Pharmacol. 2006; 70(5):1630. [PubMed: 16880288]
10. Quick M, et al. State-dependent conformations of the translocation pathway in the tyrosine transporter Tyt1, a novel neurotransmitter:sodium symporter from Fusobacterium nucleatum. J Biol Chem. 2006; 281(36):26444. [PubMed: 16798738]
11. Forrest LR, et al. Mechanism for alternating access in neurotransmitter transporters. Proc Natl Acad Sci U S A. 2008; 105(30):10338. [PubMed: 18647834]
12. Kniazeff J, et al. An intracellular interaction network regulates conformational transitions in the dopamine transporter. J Biol Chem. 2008; 283(25):17691. [PubMed: 18426798]
13. Noskov SY. Molecular mechanism of substrate specificity in the bacterial neutral amino acid transporter LeuT. Proteins. 2008; 73(4):851. [PubMed: 18536011]
14. Noskov SY, Roux B. Control of ion selectivity in LeuT: two Na^+ binding sites with two different mechanisms. J Mol Biol. 2008; 377(3):804. [PubMed: 18280500]
15. Shi L, et al. The mechanism of a neurotransmitter:sodium symporter - inward release of Na^+ and substrate is triggered by substrate in a second binding site. Mol Cell. 2008; 30(6):667. [PubMed: 18570870]
16. Singh SK. LeuT: A prokaryotic stepping stone on the way to a eukaryotic neurotransmitter transporter structure. Channels (Austin). 2008; 2(5)

17. Crisman TJ, Qu S, Kanner BI, Forrest LR. Inward-facing conformation of glutamate transporters as revealed by their inverted-topology structural repeats. Proc Natl Acad Sci U S A. 2009
18. Khalili-Araghi F, et al. Molecular dynamics simulations of membrane channels and transporters. Curr Opin Struct Biol. 2009; 19(2):128. [PubMed: 19345092]
19. Li J, Tajkhorshid E. Ion-releasing state of a secondary membrane transporter. Biophys J. 2009; 97(11):L29. [PubMed: 19948113]
20. Quick M, et al. Binding of an octylglucoside detergent molecule in the second substrate (S2) site of LeuT establishes an inhibitor-bound conformation. Proc Natl Acad Sci U S A. 2009; 106(14): 5563. [PubMed: 19307590]
21. Shi L, Weinstein H. Conformational rearrangements to the intracellular open states of the LeuT and ApcT transporters are modulated by common mechanisms. Biophys J. 99(12):L103. [PubMed: 21156121]
22. Zhao Y, et al. Single-molecule dynamics of gating in a neurotransmitter transporter homologue. Nature. 2010; 465(7295):188. [PubMed: 20463731]
23. Singh SK, Piscitelli CL, Yamashita A, Gouaux E. A competitive inhibitor traps LeuT in an open-to-out conformation. Science. 2008; 322(5908):1655. [PubMed: 19074341]
24. Claxton DP, et al. Ion/substrate-dependent conformational dynamics of a bacterial homolog of neurotransmitter:sodium symporters. Nat Struct Mol Biol. 2010; 17(7):822. [PubMed: 20562855]
25. Singh SK, Yamashita A, Gouaux E. Antidepressant binding site in a bacterial homologue of neurotransmitter transporters. Nature. 2007; 448(7156):952. [PubMed: 17687333]
26. Beckett D, Kovaleva E, Schatz PJ. A minimal peptide substrate in biotin holoenzyme synthetase-catalyzed biotinylation. Protein Sci. 1999; 8(4):921. [PubMed: 10211839]
27. Zhou Z, et al. LeuT-desipramine structure reveals how antidepressants block neurotransmitter reuptake. Science. 2007; 317(5843):1390. [PubMed: 17690258]
28. Zhou Z, et al. Antidepressant specificity of serotonin transporter suggested by three LeuT-SSRI structures. Nat Struct Mol Biol. 2009; 16(6):652. [PubMed: 19430461]
29. Sen N, Shi L, Beuming T, Weinstein H, Javitch JA. A pincer-like configuration of TM2 in the human dopamine transporter is responsible for indirect effects on cocaine binding. Neuropharmacology. 2005; 49(6):780. [PubMed: 16216288]
30. Piscitelli CL, Krishnamurthy H, Gouaux E. Neurotransmitter/sodium symporter orthologue LeuT has a single high-affinity substrate site. Nature. 468(7327):1129. [PubMed: 21179170]
31. Schaffner W, Weissmann C. A rapid, sensitive, and specific method for the determination of protein in dilute solution. Anal Biochem. 1973; 56(2):502. [PubMed: 4128882]
32. Munro JB, Altman RB, O'Connor N, Blanchard SC. Identification of two distinct hybrid state intermediates on the ribosome. Mol Cell. 2007; 25(4):505. [PubMed: 17317624]
33. Caplan DA, Subbotina JO, Noskov SY. Molecular mechanism of ion-ion and ion-substrate coupling in the Na^+-dependent leucine transporter LeuT. Biophys J. 2008; 95(10):4613. [PubMed: 18708457]

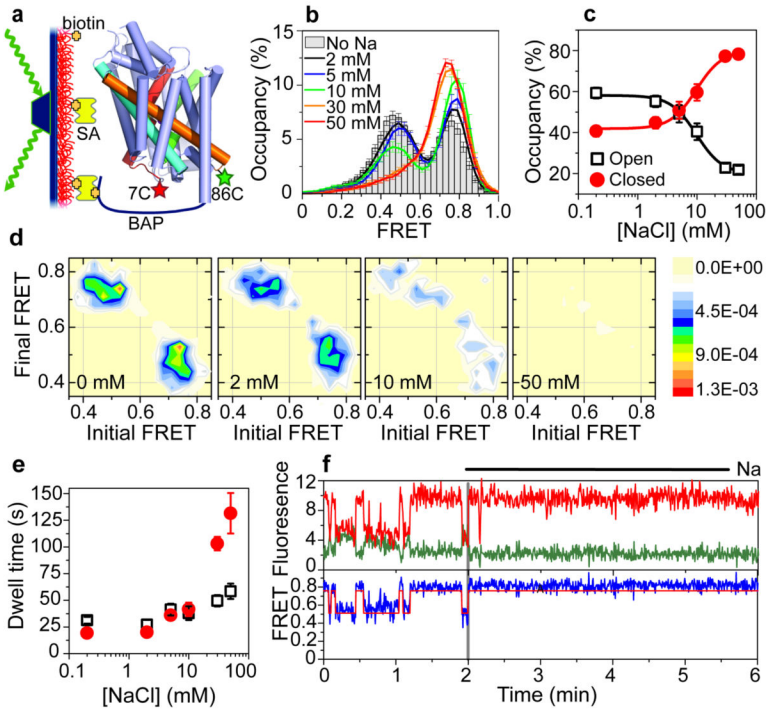

Figure 1. Effect of Na^+ on LeuT dynamics

(**a**) Experimental setup: H7C/R86C-LeuT labeled with Cy3 and Cy5 (stars) was immobilized via a biotin tag on a passivated glass surface and illuminated with total internal reflection. FRET traces (>110 per condition) were collected with varying concentrations of Na^+ (160 ms time resolution for all except 30-50 mM with 400 ms). (**b**) Histograms of FRET traces, filtered to remove fluorophore dark states. (**c**) Fraction of time in the lower-FRET open state (black open squares) and the high-FRET closed state (red filled circles). (**d**) Transition density: average FRET values before (x-axis) and after (y-axis) each transition were plotted as a histogram in transitions per second (scale at right). (**e**) Average dwell times in each state. (**f**) Representative traces (donor in green, acceptor in red, FRET in blue, and idealization in red), where the solution was exchanged at 2 min from K^+ to Na^+ (200 mM).

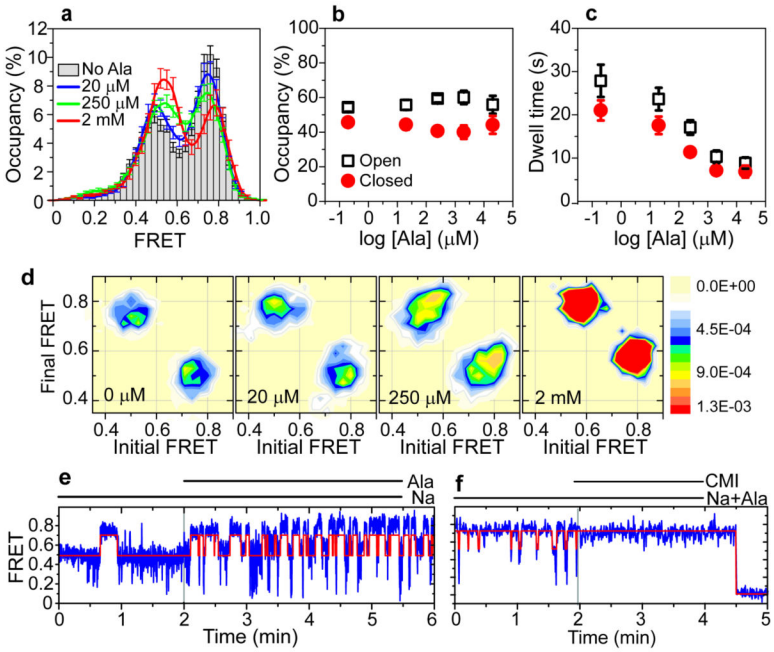

Figure 2. Effect of alanine on LeuT dynamics

smFRET traces (>90 per condition) were collected at 160 ms time resolution with 2 mM Na^+ and varying concentrations of alanine. (**a**) Histograms of FRET data from each condition. Hidden Markov modeling analysis revealed (**b**) the fraction of time and (**c**) average dwell times in the lower-FRET open state (black open squares) and the high-FRET closed state (red filled circles). (**d**) Transition density plots as in Fig. 1d. (**e-f**) Representative FRET traces (blue) with idealization (red) from experiments where solution was exchanged at 2 min: (**e**) 2 mM Na^+ adding 250 μM Ala and (**f**) 2 mM Na^+ and 250 μM Ala adding the inhibitor clomipramine (0.5 mM).

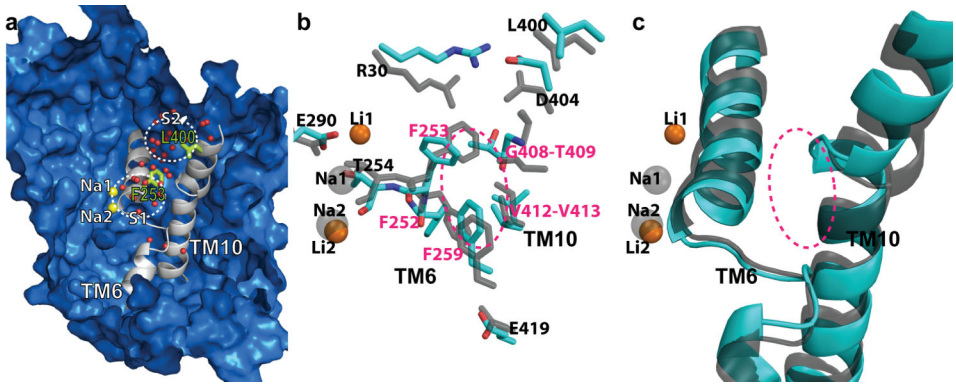

Figure 3. The configuration of TM6-TM10 interactions induced by Na^+ binding cannot be matched by Li^+

(**a**) Representative snapshot taken from the Na-only simulation, showing water molecules (red spheres) occupying the S1 and S2 sites (white dotted ellipses). Residues L400 in the S2 site and F253 in the S1 site, which were mutated to affect substrate binding, are shown as light green sticks. (**b**) The different effects that Li^+ and Na^+ binding has on the interacting residues of TM6 and TM10. The TM6/TM10 interface is indicated by the dotted ellipse in magenta. (**c**) The bulge around G408 in TM10, which is present only when Na^+ is bound but not when Li^+ replaces it. In **b** and **c,** side chains and backbones colored according to atom types are from the Li-only conformation, while those from the Na-only conformation are rendered in gray.

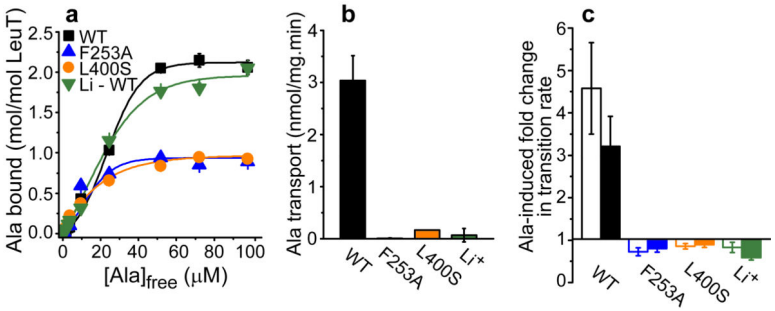

Figure 4. Effect of S1 and S2 site mutations and of Li^+ on activity and dynamics

(**a**) Binding of ^{3}H-alanine in buffer containing 50 mM Na^+ was measured for wild-type (WT, black squares), F253A (blue triangles), and L400S (orange circles) LeuT, and wild-type LeuT with 150 mM Li^+ (green inverted triangles). (**b**) Alanine uptake with 100 mM Na^+ was measured for WT (black), F253A (blue), and L400S (orange) LeuT or with 150 mM Li^+ for WT LeuT (green). (**c**) The fold change in the rate of transitioning from the open state to the closed state (open bars) and from the closed state to the open state (filled bars) induced by 250 μM Ala in 10 mM Na^+ or for WT in 40 mM Li^+ (> 280 traces and 800 transitions per condition).